Laser and Particle Beams

cambridge.org/lpb

Research Article

Cite this article: Zhang G, Xia X (2020). Laser beam self-focusing in collisional plasma with periodical density ripple. *Laser and Particle Beams* **38**, 45–53. https://doi.org/10.1017/S0263034620000026

Received: 13 August 2019
Revised: 3 January 2020
Accepted: 8 January 2020
First published online: 4 February 2020

Key words:
Collisional plasma; dielectric function; electron temperature; periodical density ripple; self-focusing

Author for correspondence:
X. Xia, College of Science, Guilin University of Technology, Guilin 541004, China. E-mail: xxpccp@163.com

Laser beam self-focusing in collisional plasma with periodical density ripple

Geng Zhang and Xiongping Xia

College of Science, Guilin University of Technology, Guilin 541004, China

Abstract

In the paper, we applied the paraxial region theory and Wentzel-–Kramers-–Brillouin approximation to study laser beam self-focusing in the interaction of laser and collisional plasma with periodical density ripple. The results have shown that, under the influence of collision nonlinear effect, laser presents stable self-focusing, self-defocusing, and oscillational self-focusing in the plasma. Besides, the parameters of plasma with periodical density ripple have a greater impact on the effect of self-defocusing and oscillational self-focusing than stable self-focusing. In certain conditions, beam self-defocusing and oscillational self-focusing would decline and even disappear, and stable self-focusing would further be strengthened. Hence, selecting a suitable periodic plasma system is advantageous for separating self-defocusing and oscillational self-focusing, and for the formation of a more stable collisional self-focusing.

Introduction

The phenomena of self-focusing in laser–plasma interactions have been researched for decades of years due to their significant advantages in various fields, such as laser particle acceleration (Faure *et al*., 2004), inertial confinement fusion (Lindl, 1995), fast ignition (Roth *et al*., 2001), and laser target (Yu *et al*., 1999), the main formation of which has been governed by different parameters in the instabilities of laser–plasma interactions. As one of the most typical nonlinear effects, different mechanisms of formation (Sharma *et al*., 2003) have been developed and temporarily identified from ponderomotive self-focusing (Max, 1976), collisional self-focusing (Perkins and Valeo, 1974), resonance self-focusing (Joshi *et al*., 1982), and relativistic self-focusing (Thakur *et al*., 2019). As an interesting and significant extension from laser–plasma interaction, the interaction in laser and plasma with periodical density ripple (Kaur *et al*., 2018) has been applied in more fields, such as THz generation (Mehta *et al*., 2019) and harmonic generation (Thakur and Kant, 2018), the definition of which mainly focuses on the comparison of the frequency in such plasmas; when the wave frequency ω is greater than electron collision frequency v, then they could be called collisional plasmas.

In experimental research, collisional plasmas have been widely found and researched in intense laser and plasma interaction. Rinderknecht *et al*. (2018) probed the structure of a strong collisional shock front formed in a plasma in laser-driven gas-jet experiments. Zhang *et al*. (2018) have investigated the collisional dynamics in femtosecond-laser-induced plasmas by using an elliptically polarized pump pulse to induce the underdense plasmas and by using a time-delayed linearly polarized probe pulse to drive the HH generation from the plasmas. Young *et al*. (2019) have investigated the low $-Z(C_5H_8O_2)$ collisional plasma jets created on the OMEGA laser.

The characters of density ripple variations in plasma have also been found and research on the process revealed more properties of interactions in plasma and matters. Guosheng *et al*. (1982) observed spontaneous periodic surface structures or ripples after illumination of various matters by intense laser pulses, which illustrated the possibility of lasers periodically pulsing on the surface of the material in the interaction between laser and the substance, providing a basis for the subsequent discovery of plasma with periodical density ripple. Min and Hora (1991) used density ripple build-up and relaxation to confirm and explain the pulsation of laser–plasma interaction. Ondarza-Rovira and Boyd (2000) observed the harmonic emission of plasma by means of particle-in-cell simulations. Garrelie *et al*. (2011) investigated the correlation between ripples formation under ultrashort laser exposure and surface plasmon polaritons generation conditions, evidencing the plasma characters of ripples generation.

In theoretical research, the main focus point of the laser–plasma interaction is focused on the field of THz laser and rippled density plasma. Bhasin and Tripathi (2009) tested a scheme of resonant THz radiation generation by optical rectification of a picosecond laser pulse in rippled density magnetized plasma. Tripathi *et al*. (2010) studied the nonlinear interaction of amplitude-modulated two- and three-dimensional laser beams with a cylindrical plasma column and the generation of terahertz (THz) radiation. Singh *et al*. (2013) presented a scheme to achieve THz radiation by the beating of cosh-Gaussian lasers in spatially periodic plasma with

https://doi.org/10.1017/S0263034620000026 Published online by Cambridge University Press

ripple density. Kumar *et al.* (2015) investigated the effect of self-focusing and defocusing on THz generation by amplitude-modulated Gaussian laser beam in rippled density plasma. Valkunde *et al.* (2018*a*, 2018*b*) have found that exponential plasma density ramp causes the laser beam to become more focused than tangent density ramp over several Rayleigh lengths in the dielectric function of plasma which has an upward density ramp of tangent and exponential profiles. Jafari Milani *et al.* (2019) have found that increasing the background electron density and considering the collision frequency could force the generation of THz in a warm rippled density plasma. Abedi and Jafari (2018) have studied the terahertz (THz) radiation generated by two Cosh–Gaussian laser beams mixed in collisional magnetized plasma in the presence of a helical magnetostatic wiggler. By calculation, their results have shown that the amplitude of THz electric field radiation increases along with the increase in wiggler frequency, the radiation as well becomes stronger. Varshney *et al.* (2018) proposed a scheme for terahertz radiation generation by using nonlinear mixing of two cosh-Gaussian laser beam in axially magnetized plasma with spatially periodic density ripple, and the results showed the amplitude of THz wave enhances with decentered parameters as well as with the magnitude of axially applied magnetic field, the amplitude is found to be highly sensitive to collision frequency. Safari *et al.* (2018) studied the nonlinear interaction of Hermite–Gaussian and Laguerre–Gaussian (LG) laser beams with a collisional inhomogeneous plasma and effects of laser beams and plasma parameters. Valkunde *et al.* (2018*a*, 2018*b*) have analytically investigated the domain of decentered parameter and its effect on the self-focusing of Hermite-cosh-Gaussian (HChG) laser beams in a collisional plasma, they obtained the nonlinear differential equation of the beam width parameter for various laser modes of HChG beam by following the standard Akhamanov's parabolic equation approach under Wentzel–Kramers–Brillouin (WKB) and paraxial approximations. The results made them to redefine three distinct regions: self-focusing, self-trapping, and defocusing, which are presented graphically.

Collision plasma with periodic density ripple have been discovered according to a certain experiment for further learning about the characters of self-focusing, especially engaged in the effect of the electron temperature on the nonlinear dielectric constant and some parameters during the laser beam propagation. In this paper, by means of the paraxial approximation, research was carried on laser beam self-focusing in collisional plasma with periodical density ripple and some new and interesting phenomena of beam self-focusing in the collisional plasma with periodical density ripple have been found.

Laser propagation basic theory in plasma with periodical density ripple

The laser wave equation governing the electronic field in the plasma can be written as

$$\nabla^2\vec{E} - \nabla(\nabla\cdot\vec{E}) = \frac{\epsilon}{c^2}\frac{\partial^2\vec{E}}{\partial t^2} \tag{1}$$

where ϵ is the dielectric constant, c is the light speed, and $\vec{E}$ is the electric field.

Applying WKB approximation and paraxial theory (Sodha *et al.*, 2009), the variation in the electric field can be represented as

$$\vec{E} = \vec{A}_0(r, z, t)\exp[i(\omega t - k_0 z)] \tag{2}$$

where ω is the wave frequency and z is the axial distance along propagation. For further approximation, the electron plasma frequency ω_p is introduced, since $\omega_p^2/\omega^2 \ll \epsilon \mathrm{In}\epsilon$, one can ignore the term $\nabla(\nabla\cdot\vec{E})$ and then substitute the electric field function into Eq. (1) with a combination of the approximation, the following can be obtained:

$$-k_0^2\vec{A}_0 - 2ik_0\frac{\partial\vec{A}_0}{\partial z} + \nabla^2\vec{A}_0 + \frac{1}{V_g}\cdot\frac{\partial\vec{A}_0}{\partial t} = \frac{\omega^2}{c^2}\epsilon\vec{A}_0 \tag{3}$$

where $k_0 = \omega\epsilon_0^{1/2}/c$ is the wave number, ϵ_0 is the initial value of dielectric constant, $V_g = k_0c^2/\omega\epsilon$ is the group velocity, and $\overrightarrow{A}_0$ is a complex function of space which can be written as

$$\vec{A}_0 = \vec{A}_0(r, z, t)\exp[-ik_0 S_0(r, z, t)] \tag{4}$$

where S_0 is the real function in the space which can be written as

$$S_0 = S_{00} + \frac{r^2}{r_0^2}S_{02} \tag{5}$$

$$S_{02} = \frac{r_0^2}{2f}\frac{df}{dz} \tag{6}$$

where r is the radial coordinate of the cylindrical coordinate system and r_0 is the initial beam width.

Introducing the retarded time τ, we assume the dimensionless retarded time $\tau' = t/\tau$, and substituting $\vec{A}_0$ into Eq. (3), the laser electronic field amplitude A'^2_0 can be obtained:

$$A'^2_0 = \frac{A_{00}^2}{f^2}\exp\left(-\frac{r^2}{r_0^2 f^2}\right)F(\tau') \tag{7}$$

where A_{00}^2 is the initial value, f is the dimensionless beam width parameter in the paraxial region, and τ' is the dimensionless retarded time. Considering the real part term in the solution of Eq. (3) can be shown in the following form:

$$2\frac{\partial S_0}{\partial z} + \left(\frac{\partial S_0}{\partial r}\right)^2 = \frac{\omega^2}{k_0^2c^2}\epsilon + \frac{1}{k_0^2\vec{A}'_0}\left(\frac{1}{r}\frac{\partial\vec{A}'_0}{\partial r} + \frac{\partial^2\vec{A}'_0}{\partial r^2}\right) \tag{8}$$

Using the partial approximation along with the direction of propagation, the dielectric function ϵ can be introduced as follows:

$$\epsilon = \epsilon_0 - \frac{r^2}{r_0^2}\epsilon_2 \tag{9}$$

where ϵ_0 is the linear part and ϵ_2 is the nonlinear part.

By substituting Eqs (5)–(7) and (9) into Eq. (8), the equation governing the beam width parameter f in the paraxial region can

https://doi.org/10.1017/S0263034620000026 Published online by Cambridge University Press

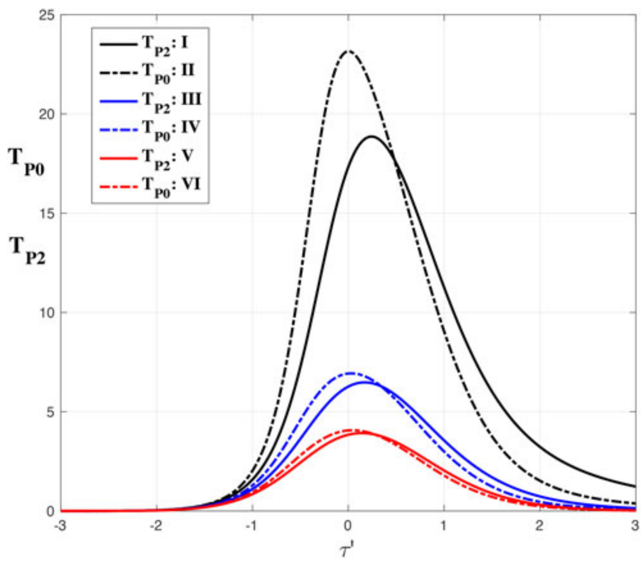

Fig. 1. Variation of axial electron temperatures T_{p0} and T_{p2} with the variations of dimensionless retarded time $\tau' = t/\tau$ for the parameters of $\delta\nu_0$ in the Gaussian pulse. $\alpha A_{00}^2 = 10$, $f = 1$, $\omega_p^2/\omega_{p0}^2 = 1 + 0.1\cos(2\pi z/3)$, $\omega_{p0}^2/\omega^2 = 0.8$, $\delta\nu_0 = 0.5$ (I), 1.5 (III), and 2.5 (V) for T_{p0}; and $\delta\nu_0 = 0.5$ (II), 1.5 (IV), and 2.5 (VI) for T_{p2}.

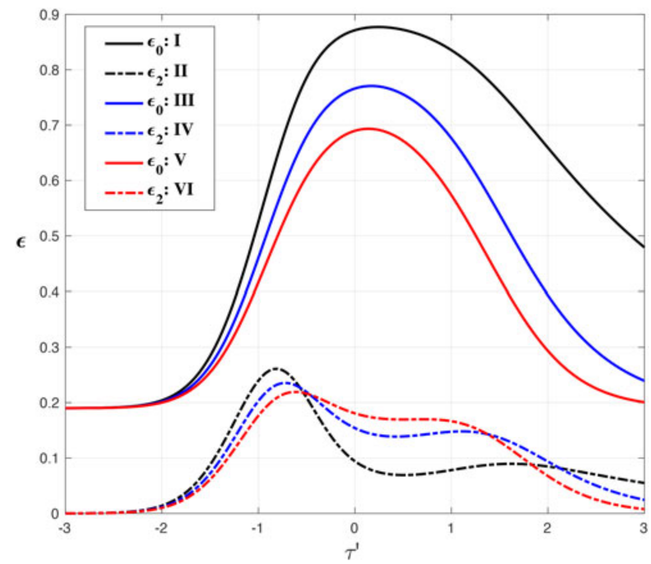

Fig. 2. Variation of axial dielectric constant (ϵ_0 and ϵ_2) with dimensionless retarded time τ' at $z = 0$ for the parameters $\delta\nu_0$ in Gaussian pulse. $\alpha A_{00}^2 = 10$, $f = 1$, $\omega_p^2/\omega_{p0}^2 = 1 + 0.1\cos(2\pi z/3)$, $\omega_{p0}^2/\omega^2 = 0.8$, $\delta\nu_0 = 0.5$ (I), 1.5 (III), and 2.5 (V) for ϵ_0, and $\delta\nu_0 = 0.5$ (II), 1.5 (IV), and 2.5 (VI) for ϵ_2.

be obtained as

$$\frac{d^2 f}{dz^2} = \frac{1}{k_0^2}\left(\frac{1}{r_0^4 f^3} - \frac{\omega^2}{c^2}\frac{f}{r_0^2}\epsilon_2\right) \tag{10}$$

For the formation of collision plasma in intense laser and matter interaction, the electrons movement function could be written as follows:

$$m\frac{d\vec{V}_e}{dt} = -e\vec{E} - m\nu_e\vec{V}_e \tag{11}$$

where m is the electronic mass, ν_e is the effective frequency of electron collisions, and $\vec{V}_e$ is the electrons drift velocity in the plasma. When substituting $\vec{V}_e$ into uniform alternating electric field $\vec{E} = \vec{E}_0\exp(i\omega t)$ with frequency ω at $t = 0$, and we assuming $t \gg 1/\nu_e$, the expression of $\vec{V}_e$ could be written as

$$\vec{V}_e = \frac{-e\vec{E}_0 e^{i\omega t}}{m(\nu_e + i\omega)} \tag{12}$$

According to thermal energy conservation, the system of plasmas including all the electrons is supported by the following:

$$\frac{d}{dt}\left(\frac{3}{2}k_B T_e\right) = -e\mathrm{Re}(\vec{E}\cdot\vec{V}_e) - \frac{3}{2}k_B\delta\nu_e(T_e - T_0) \tag{13}$$

where $-e\mathrm{Re}(\vec{E}\cdot\vec{V}_e)$ refers to the ohmic heating rate for one electron; and the latter one $-3k_B\delta\nu_e(T_e - T_0)/2$ refers to the rate of thermal energy loss in one electron during the process of collisions with other heavy particles, T_e is the electron temperature in the field, T_0 is the temperature of the plasma without the pulse, and δ is the fraction of losing excess energy during the process of collisions.

Substituting Eq. (12) into (13), one obtains

$$\frac{dT_e}{dt} + \delta\nu_e(T_e - T_0) = \frac{e^2\nu_e EE^*}{3m\omega^2 k_B} \tag{14}$$

The wave frequency $\omega \gg \nu$, where ν is the electron collision frequency, then the profile of the Gaussian function might by expressed as

$$EE^* = A_0'^2\exp\left(-\frac{r^2}{r_0^2}\right)F(\tau') \tag{15}$$

where r is the radial coordinate of the cylindrical coordinate system and r_0 is the initial beam width.

In the paraxial region, the electron temperature in the field T_e can be expressed as

$$T_e = T_0(1 + T_p) \tag{16}$$

where T_p is the dimensionless temperature, thermal energy conservation can be gained as

$$\begin{aligned}\frac{dT_p}{d\tau'} &+ \delta\nu_0\tau(1 + T_p)^{1/2}T_p \\ &= \frac{\tau\nu_0}{T_0}\frac{e^2}{3m\omega^2 k_B}\times(1 + T_p)^{1/2}\frac{A_{00}^2}{f^2}e^{-(r^2/r_0^2 f^2)}F(\tau')\end{aligned} \tag{17}$$

The dimensionless temperature T_p can be expanded as the second-order formula approximation along the axial direction of propagation distance r:

$$T_P \approx T_{P0} - \frac{r^2}{r_0^2}T_{P2} \tag{18}$$

https://doi.org/10.1017/S0263034620000026 Published online by Cambridge University Press

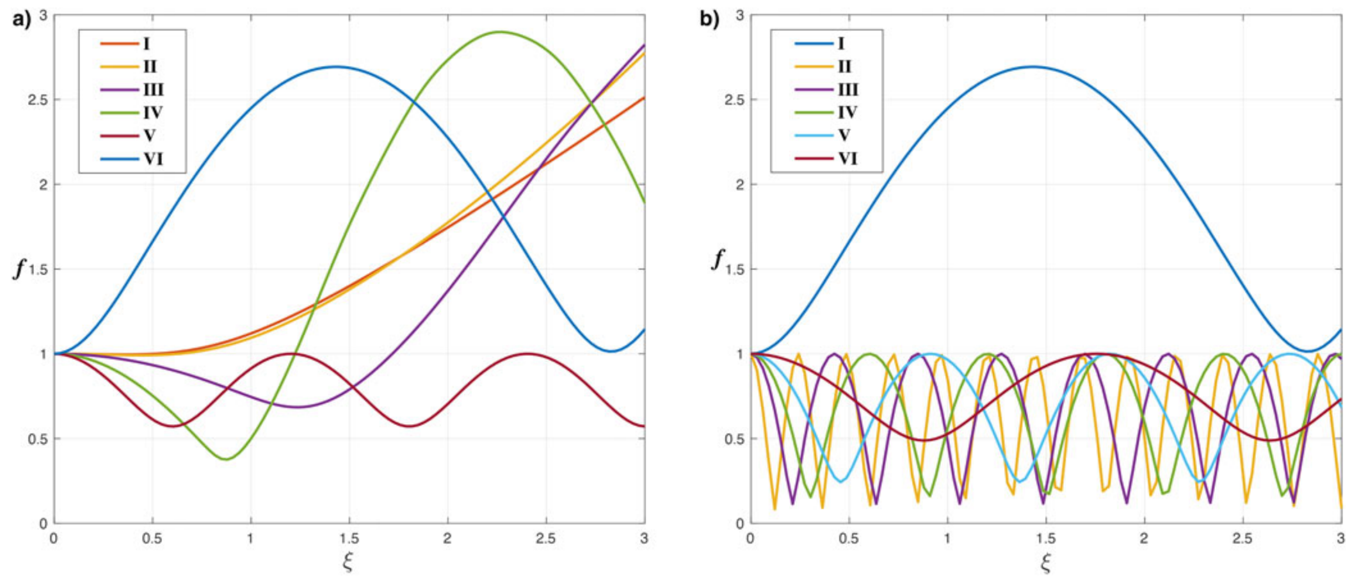

Fig. 3. Variation of width parameter f with dimensionless distance of propagation ξ for the dimensionless retarded time τ′ in Gaussian pulse. $\alpha A_{00}^2 = 10$, $f = 1$, $\omega_p^2/\omega_{p0}^2 = 1 + 0.1\cos(2\pi z/3)$, and $\omega_{p0}^2/\omega^2 = 0.8$ at τ′ = −2.5 (I), −2 (II), −1.5 (III), −1 (IV), −0.5 (V), and 0 (VI) for (a), and τ′ = 0 (I), 0.5 (II), 1 (III), 1.5 (IV), 2 (V), and 2.5 (VI) for (b).

Submitting T_p above into Eq. (17), and equating the coefficients of r^2 and r_0^2 on both sides of the equation, the following can be obtained:

$$\frac{dT_{p0}}{d\tau'} + \delta\nu_0\tau\left(T_{p0} + \frac{1}{2}T_{p0}^2\right) = \frac{\tau\nu_0}{T_0}\frac{e^2}{3m\omega^2 k_B}\frac{A_{00}^2}{f^2} \times \left(1 + \frac{T_{p0}}{2}\right)F(\tau') \tag{19}$$

$$\frac{dT_{p2}}{d\tau'} + \delta\nu_0\tau(T_{p0}T_{p2} + T_{p2}) = \frac{\alpha A_{00}^2}{f^2}\left[\frac{T_{p0}}{2} + \frac{1}{f^2}\left(1 + \frac{T_{p0}}{2}\right)\right]F(\tau') \tag{20}$$

$$\alpha = e^2\tau\nu_0/3m\omega^2 k_B T_0 \tag{21}$$

The two second-order non-homogeneous differential equations have introduced the dimensionless variable of temperature T_p in plasma with periodical density ripple, and with which the extensions T_{p0} and T_{p2}, the temperatures particularly depend on the dimensionless retarded time τ′.

By using the coordinate conversion, we introduce the dimensionless distance of propagation

$$\xi = zc(\omega r_0^2) \tag{22}$$

and the dimensionless initial beam width

$$\beta = r_0\omega/c \tag{23}$$

The dielectric function ϵ as shown in Eq. (9) has the linear part ϵ_0 and the nonlinear part ϵ_2 which can be expanded and the electron plasma frequency and the electron temperature can be applied:

$$\epsilon_0 = 1 - \frac{\omega_p^2}{\omega^2}\frac{2}{2 + T_{p0}} \tag{24}$$

$$\epsilon_2 = \frac{\omega_p^2}{\omega^2}\frac{2T_{p2}}{(2 + T_{p0})^2} \tag{25}$$

Substituting Eqs (22)–(25) with the wavenumber $k_0 = \omega\epsilon_0^{1/2}/c$ into Eq. (10), the modified equation of the beam width in the paraxial region could be obtained:

$$\frac{d^2f}{d\xi^2} = \frac{2 + T_{p0}}{2 + T_{p0} - 2\omega_p^2/\omega^2}\frac{1}{f^3} - \frac{2T_{p2}\omega_p^2/\omega^2}{(2 + T_{p0})(2 + T_{p0} - 2\omega_p^2/\omega^2)}\beta^2 f \tag{26}$$

The equation of the beam width mainly depends on the temperature of the electron and spatial–temporal coordinate parameters. On the right part, the first term refers to the beam diffraction and the later one represents the nonlinear part of the laser–plasma interaction system.

According to previous researches (Xia, 2014), the relations between electron density and electron frequency can be expressed as $n_e/n_{e0} = \omega_p^2/\omega_{p0}^2$, where ω_p is the electron plasma frequency for the interactions with the laser beam. So Eq. (26) in inhomogeneous collisional plasmas can be changed into the following

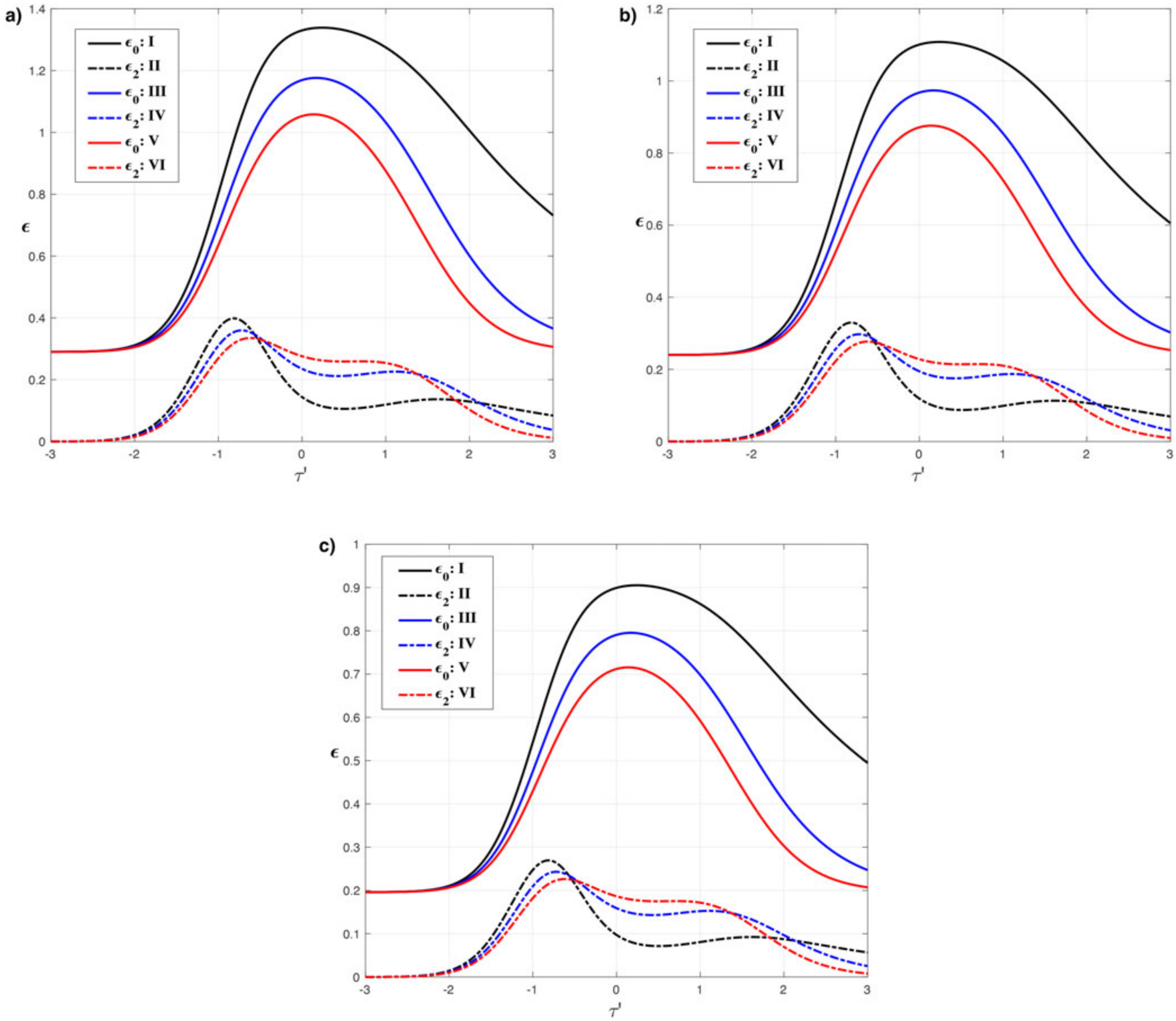

Fig. 4. Variation of axial dielectric constant (ϵ_0 and ϵ_2) with dimensionless retarded time τ' at $z = 0$ for the parameters δv_0 in Gaussian pulse. $\alpha A_{00}^2 = 10$, $f = 1$, $\omega_{p0}^2/\omega^2 = 0.8$, $\delta v_0 = 0.5$ (I), 1.5 (III), and 2.5 (V) for ϵ_0, and $\delta v_0 = 0.5$ (II), 1.5 (IV), and 2.5 (VI) for ϵ_2 in (a), (b), and (c), $\omega_p^2/\omega_{p0}^2 = 1.5 + 0.1\cos(2\pi z/3)$ for (a), $1.5 + 0.6\cos(2\pi z/3)$ for (b), and $1.5 + 0.6\cos(5\pi z/6)$ for (c).

form:

$$\frac{d^2 f}{d\xi^2} = \frac{2 + T_{p0}}{2 + T_{p0} - 2(\omega_p^2/\omega_{p0}^2) \times (\omega_{p0}^2/\omega^2)} \frac{1}{f^3} - \frac{2T_{p2}(\omega_p^2/\omega_{p0}^2) \times (\omega_{p0}^2/\omega^2)}{(2 + T_{p0})(2 + T_{p0} - 2(\omega_p^2/\omega_{p0}^2) \times (\omega_{p0}^2/\omega^2))} \beta^2 f \quad (27)$$

Collisional plasma with periodic density ripple have been found according to the experiment. In this paper, the collisional plasmas are assumed as $n_e/n_{e0} = A + B\cos(Cz)$, where A refers to the rate of electron density and initial electron density, B is the rippled parameter of collisional plasma, respectively, and c is the wave number.

Numerical results and discussions

According to the above analysis, during the interaction in laser and plasma with periodical density ripple, numerical calculations for Eqs (19), (20), (24), (25), and (27) yielded a relationship between electron temperature, dielectric constants, and beam width. The relevant parameters are specified in Figures 1–6.

Figure 1 shows the electron temperatures T_{p0} and T_{p2} as a function of dimensionless retarded time $\tau' = t/\tau$. On the whole, both the values of T_{p0} and T_{p2} increase first and then decrease, showing a single peak. In addition, with δv_0 increasing, the amplitudes of T_{p0} and T_{p2} decrease. While T_{p0} and T_{p2} do not reach the peak values at the same time. In addition, with the increase in δv_0, peak values of both T_{p0} and T_{p2} have decreased.

Figure 2 shows the variation of the dielectric constants ϵ_0 and ϵ_2 along with the dimensionless retarded time τ' in different pulse widths at $\xi = 0$. It is shown that ϵ_0 and ϵ_2 have shown the obvious

https://doi.org/10.1017/S0263034620000026 Published online by Cambridge University Press

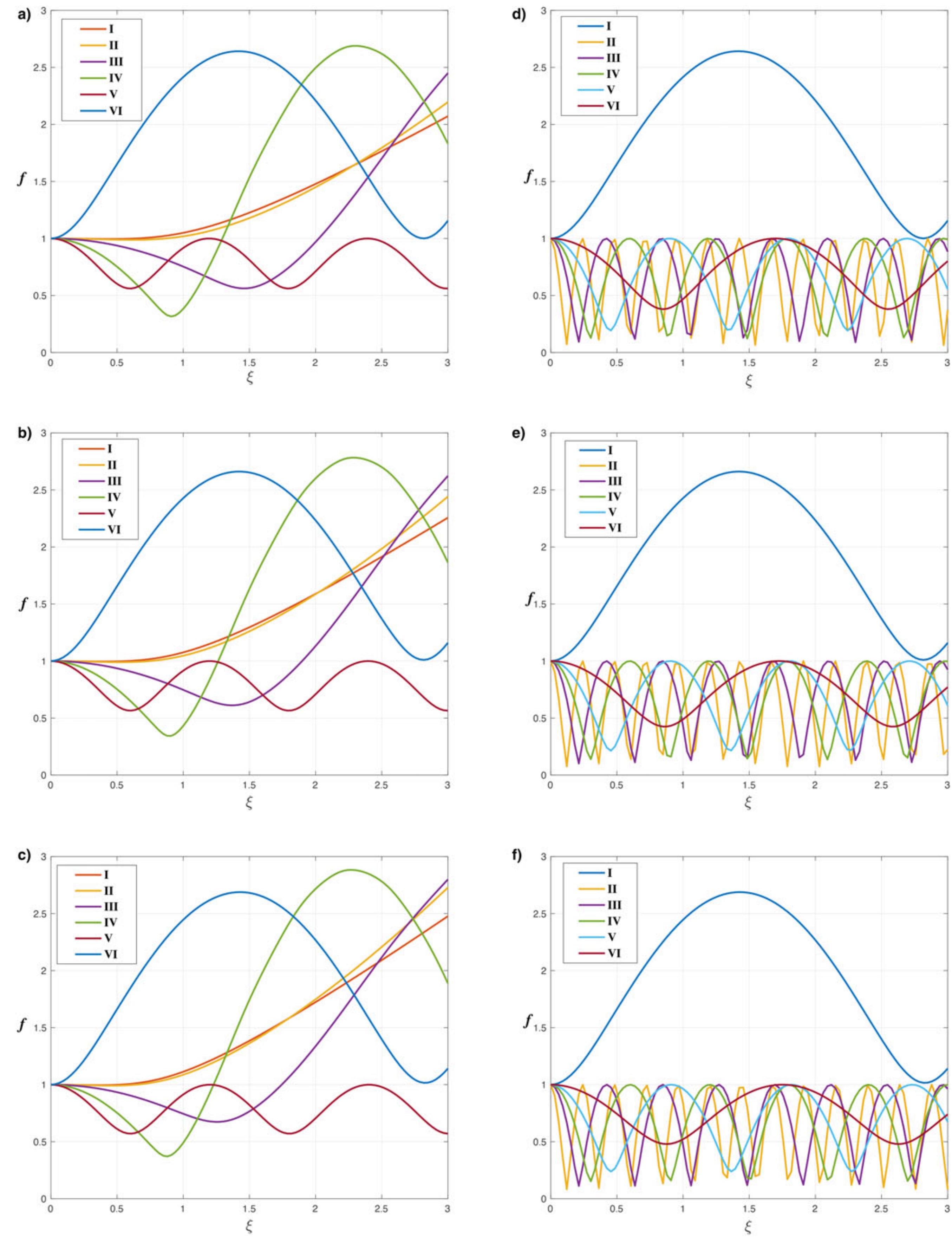

Fig. 5. Variation of width parameter f with dimensionless distance of propagation ξ for the dimensionless retarded time τ' in Gaussian pulse. $\alpha A_{00}^2 = 10$, $f = 1$, $\omega_{p0}^2/\omega^2 = 0.8$ at $\tau' = -2.5$ (I), -2 (II), -1.5 (III), -1 (IV), -0.5 (V), and 0 (VI) for (a), (b), and (c), and $\tau' = 0$ (I), 0.5 (II), 1 (III), 1.5 (IV), 2 (V), and 2.5 (VI) for (d), (e), and (f), and $\omega_p^2/\omega_{p0}^2 = 1.5 + 0.1\cos(2\pi z/3)$ for (a) and (d), $1.5 + 0.6\cos(2\pi z/3)$ for (b) and (e), and $1.5 + 0.6\cos(5\pi z/6)$ for (c) and (f).

https://doi.org/10.1017/S0263034620000026 Published online by Cambridge University Press

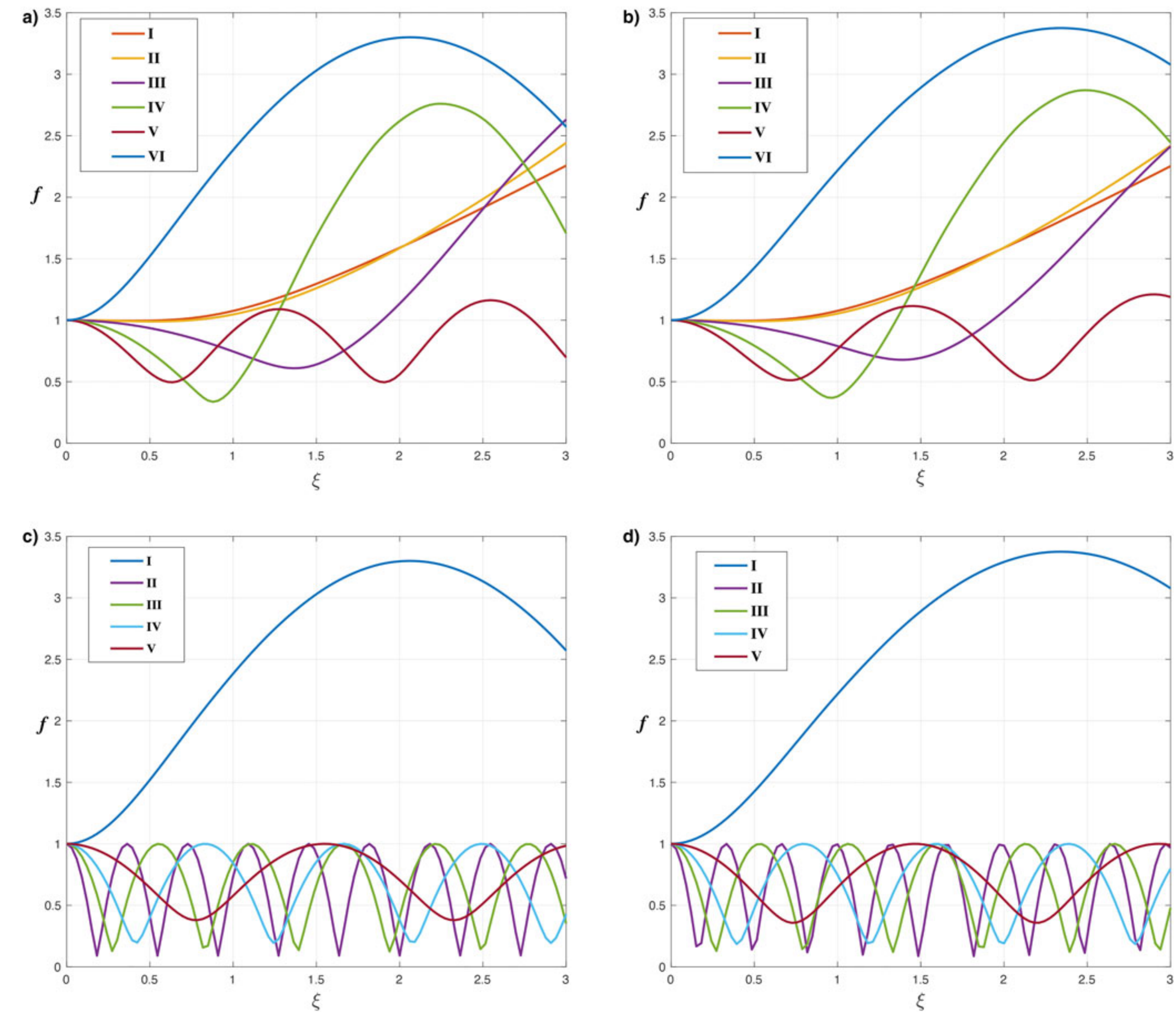

Fig. 6. Variation of width parameter f with dimensionless distance of propagation ξ for the dimensionless retarded time τ' in Gaussian pulse. $\alpha A_{00}^2 = 15$, $\omega_p^2/\omega_{p0}^2 = 1.5 + 0.6\cos(2\pi z/3)$, and $\omega_{p0}^2/\omega^2 = 0.8$ at $\tau' = -2.5$ (I), -2 (II), -1.5 (III), -1 (IV), -0.5 (V), and 0 (VI) for (a) and (b), and $\tau' = 0$ (I), 0.5 (II), 1 (III), 1.5 (IV), 2 (V), and 2.5 (VI) for (c) and (d), $f = 1$ for (a) and (c), as well as $f = 0.8$ for (b) and (d).

oscillatory during the dimensionless retarded time, besides the linear part ϵ_0 is always larger than the nonlinear part ϵ_2, and ϵ_2 is relatively more complex than ϵ_0. This is because that the electron temperature and density varied under the influence of collisional nonlinear effect, leading to the nonlinear variations of the dielectric function. Additionally, it shows that the peak values of ϵ_0 and ϵ_2 decrease steadily with the increase in losing excess energy factor $\delta\nu_0$. This is because effective collision decreases with the increase of $\delta\nu_0$, leading to the peak of dielectric function on decline.

Figure 3 shows the variation of the dimensionless beam width parameter f with the variation of the dimensionless distance of propagation ξ for different values of the dimensionless retarded time τ'. In Figure 3, in plasma with periodical density ripple, laser beam presents three obvious nonlinear phenomena, which are self-defocusing [see Fig. 3a(I–III)], oscillational self-focusing [see Fig. 3a(IV and VI) and 3b(I)], and stable self-focusing [see Fig. 3a(V) and 3b(I–IV and VI)] in different dimensionless retarded time τ'. This is actually the competition results between the convergence term caused by nonlinearity and the discrete term generated by diffraction, such a competitive mechanism leads to stable self-focusing when the convergence term is greater than the discrete term, and self-focusing with oscillational variation when the convergence term has similar degree with the discrete term, and self-defocusing when the convergence term is less than the discrete term. In the initial stage, due to the obvious diffraction effect, self-defocusing and oscillational self-focusing mainly occur. The effect of the collision nonlinearity is significantly strengthened with time, in this case, the convergence term caused by the collision nonlinearity is enhanced, resulting in the significantly enhanced stable self-focusing, while the other two are weakened or even disappear.

Figure 4 reflects the variations in the dielectric function in different plasmas with periodic density distributions. Comparing

https://doi.org/10.1017/S0263034620000026 Published online by Cambridge University Press

with Figure 2, with the increase in the rate of electron density and initial electron density A in (a), the amplitude of the dielectric function is significantly larger, based on the profile in (a), when increasing the rippled parameter of collisional plasma B in (b), the whole amplitude will be slightly reduced. And then increasing the wave number c in (c), the amplitude of the plasma dielectric constant is restored to a reduced level. This is because when the density increases, the frequency of electron collision increases, and the dielectric function increases as well. With the strengthening of B and c, the variation of fluctuation increases and the dielectric function decreases.

Figure 5 discusses the effect on beam width in plasmas with different parameters. Specifically, compared with (a) in Figure 3, it can be seen with Figure 5a as well, when increasing A, the maximum amplitude of the curve with a larger amplitude is slightly lower, the other different curves seem to be without any variations. From (a), (b), (d), and (e), when increasing B, there are relatively obvious variations in the amplitude which occur on the curve with a larger amplitude and which become larger again. When increasing c, as is shown in (b) and (c), it could be observed that the curve with a larger amplitude has a slightly larger maximum value, the change of the ratio curve is not obvious, and (d) is similar to the change of (e), and most of the amplitudes are still at the low level, the wavelength is basically stabilized. The possible reason for the above phenomenon is that under the influence of collision nonlinear factors, the parameters of plasma with periodical density ripple have a greater impact on the effect of self-defocusing and self-focusing with oscillational variation than the stable self-focusing.

Figure 6 shows the effects of variations in the beam width parameter from $f = 1$ to $f = 0.8$ during the propagation. When $f = 1$ in (a) and (c), it can be found that there are several phenomena here, forming stable self-focusing [VI in (a), and II, III, IV, and V in (c)], self-focusing with oscillational variations [I and V in (a), and I in (c)], and self-defocusing phenomenon [III, IV, and V in (a)]. Obviously, the parameter f has a significant effect on self-defocusing and oscillational self-focusing. As f decreases, amplitudes of the two nonlinear phenomena increase slightly, while self-focusing becomes faster on the same length.

Conclusion

According to the latest experimental results about the plasma with periodical density ripple, in the paper, we applied the paraxial region theory and WKB approximation to study the self-focusing in laser and plasma with periodical density ripple. Under the influence of the collision nonlinearity effect, the electronic temperature and the dielectric function present obvious nonlinear oscillatory variations and lead to three nonlinear phenomena, where laser presents stable self-focusing, self-defocusing, and oscillational self-focusing in plasma with periodical density ripple. Under the combined influence of collision nonlinear effect and periodical density ripple, stable self-focusing will dominate with time. Especially by changing the parameters of periodical density ripple, the three kinds of nonlinear phenomena will be further affected, and these parameters have a greater impact on self-defocusing and oscillational self-focusing. Hence, selecting a suitable periodic plasma system is advantageous for separating self-defocusing and self-focusing with oscillational variation, and thereby forming a more stable collisional self-focusing.

Financial support. The work is supported by the National Natural Science Foundation of China (Grant No. 11447169), the Natural Science Foundation of Guangxi province (2018|GXNSFAA138180, 2016|GXNSFAA380071, 2016GXNSFBA380204).

References

Abedi-Varaki M and Jafari S (2018) Enhanced THz radiation from beating of two Cosh–Gaussian laser beams in a wiggler-assisted collisional magnetized plasma. *Journal of the Optical Society of America B* **35**, 1165–1172.

Bhasin L and Tripathi VK (2009) Terahertz generation via optical rectification of x-mode laser in a rippled density magnetized plasma. *Physics of Plasmas* **16**, 103105.

Faure J, Glinec Y, Pukhov A, Kiselev S, Gordienko S, Lefebvre E, Rousseau JP, Burgy F and Malka V (2004) A laser–plasma accelerator producing monoenergetic electron beams. *Nature* **431**, 541–544.

Garrelie F, Colombier JP, Pigeon F, Tonchev S, Faure N, Bounhalli M, Reynaud S and Parriaux O (2011) Evidence of surface plasmon resonance in ultrafast laser-induced ripples. *Optics Express* **19**, 9035–9043.

Guosheng Z, Fauchet PM and Siegman AE (1982) Growth of spontaneous periodic surface structures on solids during laser illumination. *Physical Review B* **26**, 5366.

Jafari Milani MR, Rezaei S and Jafari MJ (2019) Effects of the evolution of two cross-focused Gaussian laser beams on the terahertz generation in thermal collisional plasma. *Contributions to Plasma Physics* **59**, 292–303.

Joshi C, Clayton CE and Chen FF (1982) Resonant self-focusing of laser light in a plasma. *Physical Review Letters* **48**, 874.

Kaur M, Agarwal PC, Kaur S and Gill TS (2018) Relativistic effects on propagation of q-Gaussian laser beam in a rippled density plasma: application of higher order corrections. *Laser and Particle Beams* **36**, 246–253.

Kumar S, Singh RK, Singh M and Sharma RP (2015) THz radiation by amplitude-modulated self-focused Gaussian laser beam in ripple density plasma. *Laser and Particle Beams* **33**, 257–263.

Lindl J (1995) Development of the indirect-drive approach to inertial confinement fusion and the target physics basis for ignition and gain. *Physics of Plasmas* **2**, 3933.

Max CE (1976) Strong self-focusing due to the ponderomotive force in plasmas. *Physics of Fluids* **19**, 74–77.

Mehta A, Kant N and Vij S (2019) Generation of terahertz (THz) radiation by p-polarised lasers beating in hot plasma with surface density ripple. *Laser Physics Letters* **16**, 045403.

Min G and Hora H (1991) Pulsation of laser–plasma interaction explained by density ripple buildup and relaxation for understanding smoothing by random-phase plate, ISI, and broadband. *Laser and Particle Beams* **9**, 381–395.

Ondarza-Rovira R and Boyd TJM (2000) Plasma harmonic emission from laser interactions with dense plasma. *Physics of Plasmas* **7**, 1520–1530.

Perkins FW and Valeo EJ (1974) Thermal self-focusing of electromagnetic waves in plasmas. *Physical Review Letters* **32**, 1234.

Rinderknecht HG, Park HS, Ross JS, Amendt PA, Higginson DP, Wilks SC, Haberberger D, Katz J, Froula HD, Hoffman MN, Kagan G, Keenan DB and Vold LE (2018) Highly resolved measurements of a developing strong collisional plasma shock. *Physical Review Letters* **120**, 095001.

Roth M, Cowan TE, Key MH, Hatchett SP, Brown C, Fountain W, Johnson J, Pennington MD, Snavely AR, Wilks CS, Yasuike K, Ruhl H, Pegoraro F, Bulanov SV, Campbell EM, Perry MD and Powell H (2001) Fast ignition by intense laser-accelerated proton beams. *Physical Review Letters* **86**, 436.

Safari S, Niknam AR, Jahangiri F and Jazi B (2018) Terahertz radiation generation through the nonlinear interaction of Hermite and Laguerre Gaussian laser beams with collisional plasma: field profile optimization. *Journal of Applied Physics* **123**, 153101.

Sharma A, Prakash G, Verma MP and Sodha MS (2003) Three regimes of intense laser beam propagation in plasmas. *Physics of Plasmas* **10**, 4079–4084.

Singh M, Singh RK and Sharma RP (2013) THz generation by cosh-Gaussian lasers in a rippled density plasma. *Europhysics Letters* **104**, 35002.

Sodha MS, Faisal M and Verma MP (2009) Effect of self-focusing on third harmonic generation by a Gaussian beam in a collisional plasma. *Physics of Plasmas* **16**, 082304.

Thakur V and Kant N (2018) Exponential density transition-based enhanced second harmonic generation in plasma. *Laser and Particle Beams* **36**, 363–368.

Thakur V, Wani MA and Kant N (2019) Relativistic self-focusing of Hermite-cosine-Gaussian laser beam in collisionless plasma with exponential density transition. *Communications in Theoretical Physics* **71**, 736.

Tripathi D, Bhasin L, Uma R and Tripathi VK (2010) Terahertz generation by an amplitude-modulated Gaussian laser beam in a rippled density plasma column. *Physica Scripta* **82**, 035504.

Valkunde AT, Patil SD, Takale MV, Vhanmore BD, Urunkar TU, Gavade KM and Gupta DN (2018*a*) Exponential density transition based self-focusing of Gaussian laser beam in collisional plasma. *Optik* **158**, 1034–1039.

Valkunde AT, Patil SD, Vhanmore BD, Urunkar TU, Gavade KM, Takale MV and Fulari VJ (2018*b*) Analytical investigation on domain of decentered parameter for self-focusing of Hermite-cosh-Gaussian laser beam in collisional plasma. *Physics of Plasmas* **25**, 033103.

Varshney P, Upadhayay A, Madhubabu K, Sajal V and Chakera JA (2018) Strong terahertz radiation generation by cosh-Gaussian laser beams in axially magnetized collisional plasma under non-relativistic ponderomotive regime. *Laser and Particle Beams* **36**, 236–245.

Xia X (2014) Nonlinear structure of electromagnetic field, electron temperature and electron density in interaction of relativistic laser and plasma with density ripple. *Laser and Particle Beams* **32**, 591–597.

Young RP, Kuranz CC, Froula D, Ross JS and Klein S (2019) Observation of collisionless-to-collisional transition in colliding plasma jets with optical Thomson scattering. *Physics of Plasmas* **26**, 012101.

Yu J, Jiang Z, Kieffer JC and Krol A (1999) Hard x-ray emission in high intensity femtosecond laser–target interaction. *Physics of Plasmas* **6**, 1318.

Zhang L, Wei P, Qin M, Yuan X, Liu C, Geng T, Zhu H, Duan Y, Zhuang S, Lu P and Kim DE (2018) Collisional dynamics in laser-induced plasmas: evidence for electron-impact excitation. *Optics Express* **26**, 10392–10399.